



HAL
open science

Development and evaluation of a new procedure for subject-specific tensioning of finite element knee ligaments

Bhriku K. Lahkar, Pierre-Yves Rohan, Helene Pillet, Patricia Thoreux, Wafa Skalli

► **To cite this version:**

Bhriku K. Lahkar, Pierre-Yves Rohan, Helene Pillet, Patricia Thoreux, Wafa Skalli. Development and evaluation of a new procedure for subject-specific tensioning of finite element knee ligaments. *Computer Methods in Biomechanics and Biomedical Engineering*, 2021, 24 (11), pp.1195-1205. 10.1080/10255842.2020.1870220 . hal-03479650

HAL Id: hal-03479650

<https://hal.science/hal-03479650v1>

Submitted on 14 Dec 2021

HAL is a multi-disciplinary open access archive for the deposit and dissemination of scientific research documents, whether they are published or not. The documents may come from teaching and research institutions in France or abroad, or from public or private research centers.

L'archive ouverte pluridisciplinaire **HAL**, est destinée au dépôt et à la diffusion de documents scientifiques de niveau recherche, publiés ou non, émanant des établissements d'enseignement et de recherche français ou étrangers, des laboratoires publics ou privés.



Development and evaluation of a new procedure for subject-specific tensioning of finite element knee ligaments

Journal:	<i>Computer Methods in Biomechanics and Biomedical Engineering</i>
Manuscript ID	GCMB-2020-0206.R1
Manuscript Type:	Research Article (5500 words)
Date Submitted by the Author:	n/a
Complete List of Authors:	Lahkar, Bhrgu; Arts et Metiers ParisTech, Institut de Biomécanique Humaine Georges Charpak Rohan, Pierre-Yves; Arts et Metiers ParisTech, Institut de Biomecanique Humaine Georges Charpak Pillet, Hélène; Arts et Metiers ParisTech, Institut de Biomécanique Humaine Georges Charpak Thoreux, Patricia; Arts et Metiers ParisTech, Institut de Biomécanique Humaine Georges Charpak; Université Sorbonne Paris Nord Skalli, Wafa; Arts et Metiers ParisTech, Institut de Biomécanique Humaine Georges Charpak
Keywords:	Finite Element Analysis, Ligament Prestrain, Subject-Specific Knee Model, Joint Kinematics, Model Evaluation

SCHOLARONE™
Manuscripts

1
2
3 **Research Article**
45
6
7 **Development and evaluation of a new procedure for subject-specific tensioning of**
8
9 **finite element knee ligaments**
1011
12 **AUTHORS**
1314
15 Bhrigu K. Lahkar^{1, *}, Pierre-Yves Rohan¹, Helene Pillet¹, Patricia Thoreux^{1, 2}, Wafa Skalli¹
1617
18 **AFFILIATIONS**
1920
21 ¹ *Institut de Biomécanique Humaine Georges Charpak, Arts et Métiers ParisTech, Paris,*
22
23 *France*
2425
26 ² *Université Sorbonne Paris Nord, Bobigny, France*
2728
29
30 *Corresponding author: Bhrigu K. Lahkar
3132
33 *Institut de Biomécanique Humaine Georges Charpak, Arts et Métiers ParisTech, 151*
34
35 *Boulevard de l'Hôpital, 75013 Paris, France*
3637
38 E-mail address: *bhrigu_kumar.lahkar@ensam.eu*
3940
41
42 Tel: +33 611745748
4344
45 Total Word Count (Introduction to Reference): 5452
4647
48
49 Word count (Abstract): 104
50

1
2
3 **26 Abstract**
4

5
6 **27** Subject-specific tensioning of ligaments is essential for the stability of the knee joint and
7
8 **28** represents a challenging aspect in the development of finite element models. We aimed to
9
10 **29** introduce and evaluate a new procedure for the quantification of ligament prestrains from
11
12 **30** biplanar X-ray and CT data. Subject-specific model evaluation was performed by comparing
13
14 **31** predicted femorotibial kinematics with the *in vitro* response of six cadaveric specimens. The
15
16 **32** differences obtained using personalized models were comparable to those reported in similar
17
18 **33** studies in the literature. This study is the first step towards the use of simplified, personalized
19
20 **34** knee FE models in clinical context such as ligament balancing.
21
22
23
24
25
26
27
28
29
30
31
32
33
34
35
36
37
38
39
40
41
42
43
44
45
46
47
48
49
50
51
52
53
54
55
56
57
58
59
60

37 Keywords

38 Finite Element Analysis, Ligament Prestrain, Subject-Specific Knee Model, Joint Kinematics,
39 Model Evaluation

1. Introduction

The knee joint is highly susceptible to frequent injury of ligaments. If it remains untreated, has the probability of limiting joint stability, and can further lead to progression of joint arthritis (Fleming et al. 2005). In such scenario, early stage clinical intervention e.g., ligament repair or replacement is often recommended. For such therapeutic interventions and to properly plan surgical procedures, accurate knowledge of the biomechanical behavior of knee ligaments is fundamental.

Several experiments dealing with main knee ligaments (anterior cruciate ligament (ACL), posterior cruciate ligament (PCL), lateral collateral ligament (LCL) and medial collateral ligament (MCL)) have been carried out in the literature (Gardiner et al. 2001; Yoo et al. 2010; Aunan et al. 2012; Belvedere et al. 2012; Rochcongar et al. 2016; Pedersen et al. 2019). Although these studies have substantially increased knowledge on joint functions, yet the complexity of measurements, lesser availability of cadavers, ethical and cost implications have made data acquisition challenging.

Alternatively, finite element (FE) models are commonly used as a reliable complementary means to experimental studies providing significant insight into knee joint biomechanics. A variety of modeling techniques have been utilized to model the joint structure, particularly ligaments. Some of the strategies are steered by simplicity, while others concentrate on faithful capture of specimen-specific anatomy with varying levels of joint representation fidelity. For example, some models included 3D geometries of ligaments with complex material behavior (Limbert et al. 2004; Peña et al. 2005; Kiapour et al. 2014; Orsi et al. 2016). Such approach allows to consider ligament wrapping behavior and analysis of local biomechanical response (e.g., 3D stresses and strains across tissue). Nevertheless, higher anatomically complex models require detailed image-based information of the soft tissue structures under consideration. Generation and simulation of such models often require manifold higher time than that for

1
2
3 73 simpler models (Bolcos et al. 2018). Therefore, simpler models may be beneficial for studies
4
5 74 where higher number of subjects need to be analyzed and, at the same time, capable of
6
7
8 75 predicting joint mechanics.

9
10 76 In an attempt for model simplification, other authors have proposed to represent ligaments
11
12 77 as bundles of springs or tension only cables (Moglo and Shirazi-Adl 2005; Adouni and Shirazi-
13
14 78 Adl 2009; Baldwin et al. 2012). Although ligaments are exposed to both compressive and
15
16
17 79 tensile states of stress, yet the contribution of tensile stress is substantially higher than others
18
19 80 (Peña et al. 2006; Orsi et al. 2016). Therefore, such simplification is considered reasonable and
20
21 81 recommended particularly for predicting joint kinematics (Naghibi Beidokhti et al. 2017).
22
23
24 82 Nevertheless, personalization of ligament properties (stiffness and prestrain), although
25
26 83 clinically essential to restore joint stability, yet represents a challenge for the community. For
27
28 84 example, there is a consensus that graft under-tensioning could lead to joint laxity, which is
29
30 85 biomechanically analogous to a ligament deficient knee (Sherman et al. 2012). In addition to
31
32
33 86 that, owing to variable morphology, different bundles of a ligament (e.g., two main fiber
34
35 87 bundles of ACL) may exhibit variable prestrain by becoming active at different flexion angles
36
37
38 88 (Girgis et al. 1975). From a modeling perspective, it has also been reported that incorrectly
39
40 89 applied ligament prestrain can have a considerable effect on the kinematics of the knee (Mesfar
41
42 90 and Shirazi-Adl 2006; Rachmat et al. 2016). To tackle this issue, some authors made subject-
43
44 91 specific adjustment using inverse methods to calibrate specific ligament constitutive behavior.
45
46
47 92 Models either used laxity tests (Baldwin et al. 2012; Naghibi Beidokhti et al. 2017) or
48
49 93 distraction loading (Zaylor et al. 2019) to estimate ligament properties by minimizing
50
51 94 differences between model-predicted and experimental kinetics. Such calibrations are,
52
53
54 95 however, likely to be computationally expensive.

55
56 96 In light of the above considerations, we proposed an original framework for calibrating
57
58 97 subject-specific tensioning of FE knee ligaments based on experimentally acquired data.
59
60

1
2
3 98 Subject-specific model evaluation was performed by comparing predicted femorotibial
4
5 99 kinematics under passive flexion with the experimental data of six cadaveric specimens. We
6
7
8 100 hypothesized that the employed methodology of building personalized FE models with
9
10 101 experiment-based prestrains could predict overall passive kinematics of the knee joint.

12 102 **2. Materials and methods**

14 103 The overall workflow of generating specimen-specific FE mesh is presented in figure 1

17 104 **[Figure 1 here]**

20 105 **2.1. Experimental data acquisition**

22 106 We obtained the experimental knee kinematic responses in a previous study (Rochcongar et al.
23 107 2016). The experimental procedure is recalled briefly hereafter. Six fresh-frozen lower limb
24 108 specimens harvested from subjects with age range 47 to 79 years, were tested under passive
25 109 flexion-extension on a previously validated kinematic test-bench (Hsieh and Draganich 1997;
26 110 Azmy et al. 2010). Skin and muscles were removed except eight centimeters of quadriceps
27 111 tendon and popliteus muscle prior to the kinematic data collection. All other relevant joint soft
28 112 tissue structures (such as ligaments, articular capsule) were kept intact during kinematic data
29 113 acquisition. The femur was kept fixed, and flexion movement was introduced to the tibia by a
30 114 rope and pulley system. During flexion, the positions of the three marker tripods placed on the
31 115 femur, tibia, and patella were recorded using an optoelectronic system (Polaris, Northern
32 116 Digital Inc., Canada). These recorded positions allowed establishing ancillary reference frames
33 117 (referred to as $R_{ANC_{POL}}(t)$) from $t = 0$ (before applying flexion load) till the end of flexion
34 118 (Figure 1(a)). Measurement uncertainties with the optoelectronic system was previously
35 119 assessed. Overall uncertainties of less than 0.5 mm in translational and 1° in rotational DoF
36 120 were obtained (Azmy et al. 2010).

37 121 In addition, two orthogonal radiographs of each specimen were acquired using an EOS
38 122 biplanar X-ray system (EOS, EOS-imaging, France) to obtain 3D digital models of the bones

1
2
3 123 and tripod markers. From the 3D models, anatomical reference frames (referred to as
4
5 124 $R_{ANAT_{EOS}}$) for the femur, tibia, and patella were defined (Schlatterer et al. 2009). Ancillary
6
7
8 125 reference frames (referred to as $R_{ANC_{EOS}}$) from the tripod markers were also defined allowing
9
10 126 a relationship between anatomical frames and ancillary frames, termed as M_{ANAT_ANC}
11
12 127 (Figure 1(b)). This relation was further used for converting acquired kinematic data, $R_{ANC_{POL}}$
13
14
15 128 (t) to relative patellofemoral and tibiofemoral motions in the femur anatomical reference frame
16
17 129 with Cardan sequence $ZY'X''$.

20 130 After the kinematic data acquisition, each specimen was fully dissected to identify the
21
22 131 ligament attachment sites. Absence of trauma and integrity of soft tissue structures was checked
23
24 132 during the dissection. An experienced surgeon identified the origin and insertion locations for
25
26 133 the following ligaments: anteromedial (AM) and posterolateral (PL) bundles of ACL,
27
28 134 posteromedial (PM) and anterolateral (AL) bundles of PCL, superficial (MCLs) and deep
29
30 135 (MCLd) bundles of MCL, and LCL. Identified locations were marked with radio-opaque
31
32 136 paints, and the bones were scanned using a computed tomography (CT) scanner (Philips, Best,
33
34 137 The Netherlands). 3D digital models of each dissected specimen were acquired using MITK-
35
36 138 GEM (version 5.0) giving anatomical frames ($R_{ANAT_{CT}}$) and ligament attachment sites ($P_{LIGA_{CT}}$)
37
38 139 in the CT scanner system of reference (Figure 1(c)). 3D Digital models and digital
39
40 140 footprints of ligament attachment sites were then registered into experimental initial
41
42 141 configuration. Registration was performed with biplanar X-ray data. Once the centroidal
43
44 142 coordinates of the attachment sites were known, the end-to-end distance of the ligaments origin
45
46 143 and insertion site was computed at experimental initial configuration. For the sake of
47
48 144 readability, end-to-end distance will be referred to as ligament length hereafter.

145 2.2. Initial bone pose estimation

1
2
3 146 Relative pose (position and orientation) of tibia and patella w.r.t. the femur at initial unloaded
4
5 147 configuration was obtained using the relation M_{ANAT_ANC} and experimental kinematic data,
6
7
8 148 $R_{ANC_{POL}}(t)$ at time=0 (Figure 1(d)).
9

10 149 **2.3. Specimen specific FE model**

11 150 *2.3.1. FE mesh*

12
13 151 First, subject-specific FE hexahedral mesh for each bony segment was created based on the
14
15 152 subject-specific CT based digital models (Figure 1(e)) (Lahkar et al. 2018). Then, only the
16
17 153 surface mesh (4-noded shell element) was kept to represent bones and cartilage to reduce
18
19 154 computational cost (Germain et al. 2016). Then, mesh smoothing was performed at the articular
20
21 155 surfaces to improve the mesh quality (Taubin 1995).
22
23
24
25

26
27 156 Mesh quality was assessed using standard ANSYS mesh quality indicators: aspect ratio,
28
29 157 parallel deviation, maximum angle, Jacobian ratio, and warping factor. The surface accuracy
30
31 158 of specimen specific mesh for each specimen was compared against respective 3D digital
32
33 159 model (i.e. segmented 3D geometry from CT data) by registering Hausdorff distance expressed
34
35 160 in mean (2RMS) values.
36
37
38

39 161 *2.3.2. Knee joint FE model*

40
41 162 Bones were assumed to be isotropic linear elastic with Young's modulus of 12000 MPa (Choi
42
43 163 et al. 1990). As the loading pattern in the study is quasi-static, cartilage was assumed as single-
44
45 164 phase linear isotropic material (Eberhardt et al. 1990). Cartilage regions were modeled as
46
47 165 cortico-cartilage material and assigned with Young's modulus of 250 MPa to summarize the
48
49 166 material properties of cortical bone and cartilage (Germain et al. 2016). A very thin strip of
50
51 167 material between bones and cortico-cartilage region were also modeled with intermediate
52
53 168 properties (2000 MPa) to limit mechanical discontinuity (Germain et al. 2016) (Figure 2).
54
55
56
57

58 169 **[Figure 2 here]**

1
2
3 170 Attachment sites for the cruciate and collateral ligaments were based on the already
4
5 171 identified locations (Rochcongar et al. 2016). For other ligaments and tendons (femoro-patellar
6
7 172 ligament, patellar tendon, quadriceps tendon, posterior capsule), general anatomical sites based
8
9 173 on *a priori* knowledge of an anatomist were used. Each cruciate ligament was represented by
10
11 174 2 bundles (Blankevoort and Huiskes 1991) along with MCL (deep and superficial) (Smith et
12
13 175 al. 2016). Posterior capsule and femoropatellar ligaments were each represented by 8 bundles
14
15 176 (4 bundles in the medial and lateral side each), while quadriceps and patellar tendon as 4
16
17 177 bundles each (Germain et al. 2016) and LCL as one (Meister et al. 2000). All ligaments and
18
19 178 tendons were represented as point-to-point, tension-only cable elements as their contribution
20
21 179 in tension is much higher than that in compression (Baldwin et al. 2009; Harris et al. 2016).
22
23 180 Three frictionless surface-to-surface contact pairs were considered: tibia-femur cartilage
24
25 181 (medial and lateral) and femur-patella cartilage with augmented penalty solution algorithm.
26
27
28
29
30
31
32

33 183 2.3.3. Ligament material properties

34
35 184 Three cases of ligament prestrain values ($\% \epsilon$) were considered for cruciate and collateral
36
37 185 ligaments. No prestrain values for other ligaments were considered and stiffness (k) values for
38
39 186 all the ligaments were adopted or estimated from our previous study (Germain et al. 2016). It
40
41 187 is to be noted that constant stiffness values were applied across all specimens.
42
43
44

45 188 [Figure 3 here]

46
47 189 **Case 1: Generic material properties.** Prestrain values for ACL (5%), PCL (-3%), MCL (0%)
48
49 190 and LCL (0%) were adopted from previous study (Germain et al. 2016).
50

51
52 191 **Case 2: Automatic pre-computation from experimental data.** For each specimen, ligament
53
54 192 and bundle specific prestrains were automatically computed from the experimental ligament
55
56 193 lengths using equation 1. This is illustrated for the MCL in figure 3.
57

58
59 194 **Case 3: Combination of automatic pre-computation and further manual adjustment.**
60

1
2
3 195 Initial values for the 7 ligament parameters (prestrains) were assigned with
4
5 196 precomputed ligament prestrains. The minimum and maximum bounds for each parameter was
6
7 197 defined from the literature (Blankevoort and Huiskes 1996; Baldwin et al. 2009). Each
8
9
10 198 parameter at a time was modified by changing the previously assigned value by roughly 10%
11
12 199 and RMS error between numerical and experimental kinematics was observed for each DOF.
13
14 200 Based on the error, a new parameter set was assigned. Thus the procedure was repeated till
15
16 201 rotational and translational RMS error became steady state. Stopping criteria was chosen as
17
18 202 change in RMS error between two consecutive iterations is less than or equal to 0.1° for
19
20
21 203 rotational and 0.1 mm for translation.

$$24 \quad 204 \quad 25 \quad 205 \quad \text{prestrain} = \left(\frac{\delta}{L}\right) * 100 = \left(\frac{L-L_0}{L}\right) * 100 \quad (1)$$

26
27
28 206 where, L is the experimental ligament length at initial configuration (before application of
29
30 207 flexion load), and L_0 is the zero-strain length at the end of flexion, with an assumption that
31
32 208 ligaments experience no force after the prescribed maximum flexion angle.

33 209 2.3.4. FE model simulation states

34
35
36
37 210 Three different configurations were defined to represent different simulation states applicable
38
39 211 to all the FE models and all cases of ligament properties. As the models are built from the
40
41 212 experimental initial configuration, the first state is referred to as (a) **no-load or stress free**
42
43 213 **configuration**. The second state corresponds to the configuration after attaining equilibrium
44
45 214 under prestrain effect, termed as (b) **initial equilibrium configuration** (or reference
46
47 215 configuration). The third state corresponds to the deformed states of the model upon application
48
49 216 of incremental rotational displacements on the tibial malleolus until 70° of flexion angle
50
51 217 (Germain et al. 2016). Knee flexion took place at the third state and referred to as (c) **current**
52
53 218 **deformed configuration**. Remaining DOFs were left unconstrained. Only geometric non-
54
55 219 linearity was considered for the model simulations.

220 2.3.5. Model evaluation: Knee joint kinematics

221 The relative position and orientation of the tibia w.r.t. femur was computed based on their
222 anatomical reference frames, as described in (Schlatterer et al. 2009) and interpreted in the
223 femur anatomical reference frame. One-to-one model evaluation was performed by comparing
224 predicted femorotibial kinematics to experimental measurements throughout flexion motion
225 for both the cases 2 and 3. Specimen specific RMS differences between model-predicted and
226 experimental measurements were computed based on values at 1° interval for a range of flexion
227 angle 0–60°. Eventually, RMS difference with experimental data was averaged for all the
228 specimens.

229 3. Results

230 3.1. Mesh quality

231 Quality of individual knee joint FE mesh showed no occurrence of error in terms of ANSYS
232 mesh quality indicators.

233 3.2. Surface representation accuracy

234 [Figure 4 here]

235 FE mesh surface accuracy for the femur, tibia, and patella w.r.t. corresponding CT surface
236 across all specimens were found less than or equal to (mean (2RMS) in mm) 0.04 (0.12), 0.06
237 (0.18) and 0.05 (0.14) respectively. Error-values are pictorially represented in figure 4 for
238 specimen 1 for the sake of example.

239 3.3. Estimation of subject-specific ligament material properties

240 3.3.1. Case 2: Based on automatic pre-computation from experimental data

241 [Table 1a and Table 1b here]

242 Estimated ligament stiffness and pre-strain values computed according to the procedure
243 described in subsection 2.3.3 (case 2) are presented in Table 1a and Table 1b, respectively.

244 Positive prestrain denotes tight condition and negative prestrain slack condition. Ligament
245 prestrains showed both ligament-specific and specimen-specific variability.

246 3.3.2. Case 3: Combination of automatic pre-computation and further manual adjustment

247 **[Table 1c here]**

248 Estimated ligament pre-strain values computed according to the procedure described in
249 subsection 2.3.3 (case 3) are presented in Table 1c. Ligament stiffness values were kept the
250 same as presented in Table 1a.

251 3.4. One-to-one validation of knee joint kinematics

252 On implementation of the generic ligament properties (case 1), only two FE models out of six
253 achieved full convergence. **Convergence in this study refers to successful attainment of**
254 **mechanical equilibrium (within a default tolerance value of ANSYS) at each load step.**

255 Predicted kinematics showed large deviation from the experimental both in magnitude and
256 trend (**not reported in this manuscript as only two models achieved convergence**). Using the
257 ligament material properties computed automatically (case 2, Table 1b), 5 models out of 6
258 achieved convergence throughout 60° of flexion.

259 **[Figure 5 and Figure 6 here]**

260 Using the ligament material properties computed automatically combined with manual
261 adjustment (case 3, Table 1c), all the FE knee models remained stable throughout the range of
262 flexion. Individual run time was approximately 13 minutes per specimen. One-to-one
263 comparison of model predicted femorotibial kinematics against corresponding *in vitro* results
264 for all specimens are presented in **Figure 5 and Figure 6 for automatically computed prestrains**
265 **and adjusted ligament prestrains respectively**. For both the cases, model kinematics for all DOF
266 are shown from the reference configuration (state-b) until the end of flexion movement.

267 **[Table 2 here]**

1
2
3 268 Table 2 summarizes the RMS difference between model-predicted and experimental
4
5 269 kinematics for the range of flexion angle 0–60° for the two cases (case 2 and case 3) of ligament
6
7 270 material properties. Since 5 models out of 6 were converged while applying automatically
8
9 271 computed ligament prestrains, differences are presented for 5 models.

12 272 4. Discussion

14 273 Subject-specific tensioning of ligaments is essential in developing personalized knee FE
15
16 274 models. In this study, we built subject-specific knee FE model with CT-based geometry and
17
18 275 evaluated a new procedure for subject-specific calibration of ligaments prestrain from biplanar
19
20 276 X-ray data. Predicted femorotibial kinematics of each model was compared to the
21
22 277 corresponding *in vitro* response for three different cases of ligament properties (prestrain).
23
24 278 First, we investigated whether the FE models with generic prestrain values can capture inter-
25
26 279 individual variability of the *in vitro* kinematics. Second, experimentally obtained prestrains
27
28 280 were recruited to the FE models and predicted kinematics were observed (case 2). Third, model
29
30 281 kinematics were observed with respect to calibrated ligament properties based on the
31
32 282 combination of pre-computed prestrains and further adjustment (case 3). For case 2, RMS
33
34 283 differences between model-predicted and experimental results for abduction/adduction and
35
36 284 external/internal rotation were less than or equal to 2.4° and 6.3° respectively. For translation
37
38 285 kinematics, the differences observed were less than or equal to 5.0 mm, 1.9 mm and 1.2 mm
39
40 286 respectively for posterior/anterior, superior/inferior, and lateral/medial motions. For case 3,
41
42 287 improvement in model kinematics was observed with RMS differences 1.5° and 5.3° for
43
44 288 abduction/adduction and external/internal rotation. Differences for posterior/anterior,
45
46 289 superior/inferior, and lateral/medial motions were 3.4 mm, 1.2 mm and 2 mm respectively.
47
48 290 These results show that the proposed methodology allows us to obtain a good first
49
50 291 approximation of the prestrain values with further manual adjustment to improve the kinematic
51
52 292 prediction.
53
54
55
56
57
58
59
60

1
2
3 293 As far as the authors are aware of, there are numerous challenges exist in determining
4
5 294 ligament prestrain. Challenges are linked to both measurement issues and modeling issues.
6
7
8 295 Measurement challenges are mainly methodological issues related to identification of ligament
9
10 296 attachment sites and determination of ligament elongation pattern during motion (Woo et al.
11
12 297 1990; Gardiner et al. 2001; Belvedere et al. 2012). Because of such difficulties, FE models in
13
14 298 general, adopt prestrain values from other studies available in the literature (Yang et al. 2010;
15
16 299 Galbusera et al. 2014). As these values are adopted from other experimental studies and not
17
18
19 300 corresponding to the specimen under consideration, thereby cannot be considered as subject-
20
21 301 specific. Optimization methods have also been extensively used to calibrate specific ligament
22
23 302 constitutive behavior. These approaches particularly used laxity tests to calibrate their models
24
25 303 (Baldwin et al. 2012; Naghibi Beidokhti et al. 2017). Such approaches are, although shown
26
27
28 304 effective to attain specimen-specific ligament properties, yet computationally expensive.

30
31 305 The current study focused on the development and evaluation of a new procedure for
32
33 306 subject-specific tensioning of FE knee ligaments. The proposed procedure builds upon data
34
35 307 previously collected during an experimental investigation conducted to identify ligament
36
37 308 (cruciate and collateral) attachment sites, and to determine the ligament elongation patterns
38
39 309 during passive knee flexion (Rochcongar et al. 2016). The FE model replicates the natural
40
41 310 ligament (cruciate and collateral) insertions since these are derived from the radio opaque paint
42
43 311 locations painted on the specimens prior to the CT-scan (figure 1). The values obtained were
44
45 312 consistent with those experimental measurements reported in the literature (Bicer et al. 2010;
46
47 313 Belvedere et al. 2012). It is worth mentioning that because of the lack of experimental data for
48
49 314 other ligaments, generic insertion sites were employed. Although, it is difficult to directly
50
51 315 compare the estimated prestrains with similar studies in literature because of variability in
52
53 316 ligament geometry and material property, yet the prestrain values were found within the range
54
55
56 317 confirmed by others (Wismans et al. 1980; Amiri et al. 2006; Zaylor et al. 2019). Also, most
57
58
59
60

1
2
3 318 of the ligaments were found in tensed state at full extension except PCL, which is overall in
4
5 319 agreement with the literature (Blankevoort and Huijkes 1991; Moglo and Shirazi-Adl 2005;
6
7 320 Guess et al. 2016). Similarly, predicted kinematic response also showed good correspondence
8
9 321 with the experimental results for all specimens. The experimental-numerical differences found
10
11 322 in this study were comparable to similar studies reported in the literature (Harris et al. 2016;
12
13 323 Naghibi Beidokhti et al. 2017). For instance, Beidokhti et al. reported an average RMS
14
15 324 difference of 3.5° and 2.8° respectively for abduction/adduction and external/internal rotations.
16
17 325 For anterior/posterior, superior/inferior and lateral/medial motions the differences were 3 mm,
18
19 326 2.3 mm and 1.6 mm respectively. It is worthwhile to mention that when generic properties were
20
21 327 used, most of the models couldn't reach convergence. As previously reported by other research
22
23 328 teams (e.g., (Schwartz et al., 2019)) focusing on the medial collateral ligament) convergence
24
25 329 difficulty appeared in this kind of models when material properties were not personalized.

30
31 330 The procedure to compute ligament prestrain directly from experimental data (Case 3)
32
33 331 provided satisfactory initial guess, based on which model estimated kinematics were already
34
35 332 in good agreement with the experimental data. As this approach appears to be computationally
36
37 333 inexpensive (15-20 sec to obtain ligament specific prestrain for a single knee model) and
38
39 334 methodologically simple, it may serve as a reliable alternative for estimating subject-specific
40
41 335 ligament prestrain values. To be noted that no direct evaluation of the ligament tensions was
42
43 336 performed in the present study. The decision to implement the current technique as an
44
45 337 alternative has to be conducted with caution. For successful implementation of this technique
46
47 338 towards clinics, exhaustive model evaluation under various loading conditions is required
48
49 339 including ligament tension and contact stress. Nevertheless, validating joint kinematics as a
50
51 340 first step could be valuable to show feasibility of the current approach.

52
53
54
55
56 341 This study contains some considerations and limitations worth highlighting. **First,**
57
58 342 while comparing with experimental kinematics, model-predicted results were shown from
59
60

1
2
3 343 reference configuration (state-b). It is an auto-equilibrated configuration under the prestrain
4
5 344 effect, which is not concurrent with initial experimental configuration and difficult to calibrate.
6
7
8 345 This results in absolute offset from the experimental kinematics (Baldwin et al. 2012), although
9
10 346 masked in relative kinematics. **Second**, we acknowledge that one of the sources of
11
12 347 discrepancies between experimental-numerical kinematics may come from model
13
14 348 simplifications and assumptions. **It is also to be noted that predicted kinematics with a**
15
16 349 **combination of initial guess from experimental data and further manual adjustment displayed**
17
18 350 **closer correspondence to *in vitro* data.** Although the difference is minimal, this may be
19
20 351 attributed to the representation of overall joint soft tissue structure with simple ligamentous
21
22 352 structures without including cartilage layers and menisci. **As the proposed methodology is not**
23
24 353 **based on current state-of-the-art approaches (such as MRI based complex models with detailed**
25
26 354 **soft tissue structures), there was difficulty to obtain subject-specific geometry of cartilage and**
27
28 355 **menisci with available imaging modalities (CT and biplanar X-ray) employed in our study.**
29
30
31 356 Such simplification, therefore doesn't hold if we are interested in more detailed local insights,
32
33 357 e.g., cartilage contact stress. However, for analysis, such as graft tensioning effect on knee
34
35 358 response while reconstructing ACL, such simplification was considered relevant (Peña et al.,
36
37 359 2005). **Third**, exclusion of meniscus may overestimate the role of the ligaments in constraining
38
39 360 the joint and providing stability (Harris et al. 2016). However, other studies reported no
40
41 361 remarkable influence of meniscus on the assessment of the knee joint kinematics, especially
42
43 362 for the flexion range 0°–90° (Amiri et al. 2006; Guess et al. 2010). **Fourth**, ligaments and
44
45 363 tendons were represented as bundles of 1D elements, which may not capture actual ligament
46
47 364 length variation, as they do not account for material continuum, fiber twisting or wrapping.
48
49 365 Yet, such simplification provides faster solutions and recommended, particularly for **the**
50
51 366 **prediction of knee kinematic parameters** (Bolkus et al., 2018; Naghibi Beidokhti et al., 2017).
52
53
54 367 **Fifth**, we chose to personalize only ligament prestrains, although stiffness values vary from
55
56
57
58
59
60

1
2
3 368 subject to subject. This consideration was based on sensitivity analyses found in literature,
4
5 369 where model predicted kinematics are proclaimed to be highly sensitive to strain state at initial
6
7 370 configuration rather than stiffness values (Wismans et al. 1980; Peña et al. 2005). Besides, the
8
9 371 models were validated only under passive flexion load, which may not imitate an in-vivo
10
11 372 situation of clinical interest, yet could be a first step of assessing the potential of the models
12
13 373 towards complex scenarios. In this contribution, a maximum flexion angle of 70° was
14
15 374 considered to calibrate the model as this range covers the most common amplitude of in-vivo
16
17 375 motion under level walking, during which ligaments offer a substantial contribution to knee
18
19 376 stability (Butler et al. 2007). However, perspective work will focus on calibrating the model
20
21 377 up to 120° of knee flexion. We acknowledge that no influence of experimental uncertainty nor
22
23 378 sensitivity of ligament attachment sites on predicted kinematics was performed. Future study
24
25 379 is necessary to asses this issue. Finally, the study was limited to six specimens due to time and
26
27 380 labor associated with CT segmentation, yet higher in number compared to other similar
28
29 381 published studies. This might limit the model at the current state for clinical translation;
30
31 382 however, it was imperative to build CT based models to minimize the impact of geometrical
32
33 383 uncertainty in model predictions.

34
35 384 In conclusion, as it was a first study to directly implement prestrain values on models
36
37 385 directly from the experiment, which may find scopes in model-based clinical studies, such as
38
39 386 planning of ligament balancing or reconstruction as it reduces complexity in model
40
41 387 development (especially ligament calibration) as well as computational cost, while maintaining
42
43 388 good correspondence with experimental data. In that aim, further model evaluation would be
44
45 389 necessary for larger specimen size and in other clinically relevant scenarios.
46
47
48
49
50
51
52
53
54
55
56

391 **Conflict of Interest**

392 None

393 Acknowledgments

394 The authors are deeply grateful to the ParisTech BiomecAM chair program on subject-specific
395 musculoskeletal modeling for financial support.

396 References

- 397 Adouni M, Shirazi-Adl A. 2009. Knee joint biomechanics in closed-kinetic-chain exercises. *Comput*
398 *Methods Biomech Biomed Engin.* 12(6):661–670.
- 399 Amiri S, Cooke D, Kim IY, Wyss U. 2006. Mechanics of the passive knee joint. Part 1: The role of the
400 tibial articular surfaces in guiding the passive motion. *Proc Inst Mech Eng Part H J Eng Med.*
401 220(8):813–822.
- 402 Aunan E, Kibsgård T, Clarke-Jenssen J, Röhrli SM. 2012. A new method to measure ligament balancing
403 in total knee arthroplasty: Laxity measurements in 100 knees. *Arch Orthop Trauma Surg.*
404 132(8):1173–1181.
- 405 Azmy C, Guérard S, Bonnet X, Gabrielli F, Skalli W. 2010. EOS® orthopaedic imaging system to study
406 patellofemoral kinematics: Assessment of uncertainty. *Orthop Traumatol Surg Res.* 96(1):28–36.
- 407 Baldwin MA, Clary C, Maletsky LP, Rullkoetter PJ. 2009. Verification of predicted specimen-specific
408 natural and implanted patellofemoral kinematics during simulated deep knee bend. *J Biomech*
409 [Internet]. 42(14):2341–2348. <http://dx.doi.org/10.1016/j.jbiomech.2009.06.028>
- 410 Baldwin MA, Clary CW, Fitzpatrick CK, Deacy JS, Maletsky LP, Rullkoetter PJ. 2012. Dynamic finite
411 element knee simulation for evaluation of knee replacement mechanics. *J Biomech* [Internet].
412 45(3):474–483. <http://dx.doi.org/10.1016/j.jbiomech.2011.11.052>
- 413 Belvedere C, Ensini A, Feliciangeli A, Cenni F, D'Angeli V, Giannini S, Leardini A. 2012. Geometrical
414 changes of knee ligaments and patellar tendon during passive flexion. *J Biomech* [Internet].
415 45(11):1886–1892. <http://www.ncbi.nlm.nih.gov/pubmed/22677336>
- 416 Bicer EK, Lustig S, Servien E, Selmi TAS, Neyret P. 2010. Current knowledge in the anatomy of the
417 human anterior cruciate ligament. *Knee Surgery, Sport Traumatol Arthrosc* [Internet]. 18(8):1075–
418 1084. <https://doi.org/10.1007/s00167-009-0993-8>
- 419 Blankevoort L, Huiskes R. 1991. Ligament-bone interaction in a three-dimensional model of the knee.
420 *J Biomech Eng* [Internet]. 113(3):263–269. <http://www.ncbi.nlm.nih.gov/pubmed/1921352>
- 421 Blankevoort L, Huiskes R. 1996. Validation of a three-dimensional model of the knee. *J Biomech*
422 [Internet]. [accessed 2019 Sep 3] 29(7):955–961.
423 <https://linkinghub.elsevier.com/retrieve/pii/0021929095001492>
- 424 Bolcos PO, Mononen ME, Mohammadi A, Ebrahimi M, Tanaka MS, Samaan MA, Souza RB, Li X,
425 Suomalainen JS, Jurvelin JS, et al. 2018. Comparison between kinetic and kinetic-kinematic driven
426 knee joint finite element models. *Sci Rep* [Internet]. [accessed 2019 Aug 29] 8(1):17351.
427 www.nature.com/scientificreports
- 428 Butler RJ, Marchesi S, Royer T, Davis IS. 2007. The Effect of a Subject-Specific Amount of Lateral

- 1
2
3 429 Wedge on Knee. *J Orthop Res* Sept. 25(June):1121–1127.
4
5 430 Choi K, Kuhn JL, Ciarelli MJ, Goldstein SA. 1990. The elastic moduli of human subchondral,
6 431 trabecular, and cortical bone tissue and the size-dependency of cortical bone modulus. *J Biomech.*
7 432 23(11):1103–1113.
8
9 433 Eberhardt AW, Keer LM, Lewis JL, Vithoontien V. 1990. An analytical model of joint contact. *J*
10 434 *Biomech Eng [Internet].* 112(4):407–413. <https://doi.org/10.1115/1.2891204>
11
12 435 Fleming BC, Hulstyn MJ, Oksendahl HL, Fadale PD. 2005. Ligament injury, reconstruction and
13 436 osteoarthritis. *Curr Opin Orthop.* 16(5):354–362.
14
15 437 Galbusera F, Freutel M, Dürselen L, D’Aiuto M, Croce D, Villa T, Sansone V, Innocenti B. 2014.
16 438 Material models and properties in the finite element analysis of knee ligaments: A literature review.
17 439 *Front Bioeng Biotechnol [Internet].* 2(NOV):1–11.
18 440 <http://journal.frontiersin.org/article/10.3389/fbioe.2014.00054/abstract>
19
20 441 Gardiner JC, Weiss JA, Rosenberg TD. 2001. Strain in the human medial collateral ligament during
21 442 valgus loading of the knee. *Clin Orthop Relat Res.*(391):266–274.
22
23 443 Germain F, Rohan PY, Rochcongar G, Rouch P, Thoreux P, Pillet H, Skalli W. 2016. Role of ligaments in
24 444 the knee joint kinematic behavior: Development and validation of a finite element model. In: Joldes
25 445 GR, Doyle B, Wittek A, Nielsen PMF, Miller K, editors. *Comput Biomech Med Imaging, Model*
26 446 *Comput.* Cham: Springer International Publishing; p. 15–26.
27
28 447 Guess TM, Razu S, Jahandar H. 2016. Evaluation of Knee Ligament Mechanics Using Computational
29 448 Models. *J Knee Surg.* 29(2):126–137.
30
31 449 Guess TM, Thiagarajan G, Kia M, Mishra M. 2010. A subject specific multibody model of the knee
32 450 with menisci. *Med Eng Phys [Internet].* [accessed 2019 Jul 24] 32(5):505–515.
33 451 <https://linkinghub.elsevier.com/retrieve/pii/S1350453310000494>
34
35 452 Harris MD, Cyr AJ, Ali AA, Fitzpatrick CK, Rullkoetter PJ, Maletsky LP, Shelburne KB. 2016. A
36 453 Combined Experimental and Computational Approach to Subject-Specific Analysis of Knee Joint
37 454 Laxity. *J Biomech Eng.* 138(8):081004.
38
39 455 Hsieh YF, Draganich LF. 1997. Knee kinematics and ligament lengths during physiologic levels of
40 456 isometric quadriceps loads. *Knee.* 4(3):145–154.
41
42 457 Kiapour A, Kiapour AM, Kaul V, Quatman CE, Wordeman SC, Hewett TE. 2014. Finite element model
43 458 of the knee for investigation of injury mechanisms: Development and validation. *J Biomech Eng.*
44 459 136(1):011002.
45
46 460 Lahkar BK, Rohan P-Y, Pillet H, Thoreux P, Skalli W. 2018. Fast subject specific finite element mesh
47 461 generation of knee joint from biplanar x-ray images. In: *Cmbbe [Internet].* [place unknown];
48 462 [accessed 2019 Aug 7].
49 463 [http://cmbbe2018.tecnico.ulisboa.pt/pen_cmbbe2018/pdf/WEB_PAPERS/CMBBE2018_paper_143.p](http://cmbbe2018.tecnico.ulisboa.pt/pen_cmbbe2018/pdf/WEB_PAPERS/CMBBE2018_paper_143.pdf)
50 464 [df](http://cmbbe2018.tecnico.ulisboa.pt/pen_cmbbe2018/pdf/WEB_PAPERS/CMBBE2018_paper_143.pdf)
51
52 465 Limbert G, Taylor M, Middleton J. 2004. Three-dimensional finite element modelling of the human
53 466 ACL: Simulation of passive knee flexion with a stressed and stress-free ACL. *J Biomech.* 37(11):1723–
54 467 1731.
55
56
57
58
59
60

- 1
2
3 468 Meister BR, Michael SP, Moyer RA, Kelly JD, Schneck CD. 2000. Anatomy and kinematics of the
4 469 lateral collateral ligament of the knee. *Am J Sports Med.* 28(6):869–878.
- 6 470 Mesfar W, Shirazi-Adl A. 2006. Biomechanics of changes in ACL and PCL material properties or
7 471 prestrains in flexion under muscle force-implications in ligament reconstruction. *Comput Methods*
8 472 *Biomech Biomed Engin [Internet].* 9(4):201–209. <https://doi.org/10.1080/10255840600795959>
- 11 473 Moglo KE, Shirazi-Adl A. 2005. Cruciate coupling and screw-home mechanism in passive knee joint
12 474 during extension-flexion. *J Biomech [Internet].* [accessed 2019 Jul 10] 38(5):1075–1083.
13 475 <https://linkinghub.elsevier.com/retrieve/pii/S0021929004002805>
- 15 476 Naghibi Beidokhti H, Janssen D, van de Groes S, Hazrati J, Van den Boogaard T, Verdonshot N. 2017.
16 477 The influence of ligament modelling strategies on the predictive capability of finite element models
17 478 of the human knee joint. *J Biomech [Internet].* [accessed 2019 Jul 12] 65:1–11.
18 479 <https://linkinghub.elsevier.com/retrieve/pii/S0021929017304529>
- 21 480 Orsi AD, Chakravarthy S, Canavan PK, Peña E, Goebel R, Vaziri A, Nayeb-Hashemi H. 2016. The effects
22 481 of knee joint kinematics on anterior cruciate ligament injury and articular cartilage damage. *Comput*
23 482 *Methods Biomech Biomed Engin.* 19(5):493–506.
- 25 483 Pedersen D, Vanheule V, Wirix-Speetjens R, Taylan O, Delpont HP, Scheys L, Andersen MS. 2019. A
26 484 novel non-invasive method for measuring knee joint laxity in four dof: In vitro proof-of-concept and
27 485 validation. *J Biomech [Internet].* 82:62–69. <https://doi.org/10.1016/j.jbiomech.2018.10.016>
- 29 486 Peña E, Calvo B, Martínez MA, Doblaré M. 2006. A three-dimensional finite element analysis of the
30 487 combined behavior of ligaments and menisci in the healthy human knee joint. *J Biomech [Internet].*
31 488 [accessed 2019 Jul 24] 39(9):1686–1701.
32 489 <https://linkinghub.elsevier.com/retrieve/pii/S0021929005002113>
- 35 490 Peña E, Martínez MA, Calvo B, Palanca D, Doblaré M. 2005. A finite element simulation of the effect
36 491 of graft stiffness and graft tensioning in ACL reconstruction. *Clin Biomech.* 20(6):636–644.
- 38 492 Rachmat HH, Janssen D, Verkerke GJ, Diercks RL, Verdonshot N. 2016. In-situ mechanical behavior
39 493 and slackness of the anterior cruciate ligament at multiple knee flexion angles. *Med Eng Phys*
40 494 *[Internet].* [accessed 2019 Jul 19] 38(3):209–215.
41 495 <https://linkinghub.elsevier.com/retrieve/pii/S1350453315002696>
- 43 496 Rochcongar G, Pillet H, Bergamini E, Moreau S, Thoreux P, Skalli W, Rouch P. 2016. A new method
44 497 for the evaluation of the end-to-end distance of the knee ligaments and popliteal complex during
45 498 passive knee flexion. *Knee [Internet].* 23(3):420–425. <http://dx.doi.org/10.1016/j.knee.2016.02.003>
- 48 499 Schlatterer B, Suedhoff I, Bonnet X, Catonne Y, Maestro M, Skalli W. 2009. Skeletal landmarks for
49 500 TKR implantations: Evaluation of their accuracy using EOS imaging acquisition system. *Orthop*
50 501 *Traumatol Surg Res.* 95(1):2–11.
- 52 502 Sherman SL, Chalmers PN, Yanke AB, Bush-Joseph CA, Verma NN, Cole BJ, Bach BR. 2012. Graft
53 503 tensioning during knee ligament reconstruction: Principles and practice. *J Am Acad Orthop Surg.*
54 504 20(10):633–645.
- 56 505 Smith CR, Vignos MF, Lenhart RL, Kaiser J, Thelen DG. 2016. The influence of component alignment
57 506 and ligament properties on tibiofemoral contact forces in total knee replacement. *J Biomech Eng*
58 507 *[Internet].* [accessed 2019 Jun 20] 138(2):021017.
59 508 <https://biomechanical.asmedigitalcollection.asme.org>

- 1
2
3 509 Taubin G. 1995. Curve and surface smoothing without shrinkage. IEEE Int Conf Comput Vis.:852–857.
4
5 510 Wismans J, Veldpaus F, Janssen J, Huson A, Struben P. 1980. A three-dimensional mathematical
6 511 model of the knee-joint. J Biomech [Internet]. [accessed 2019 Sep 9] 13(8):677–685.
7 512 <https://linkinghub.elsevier.com/retrieve/pii/0021929080903541>
8
9 513 Woo SLY, Weiss JA, Gomez MA, Hawkins DA. 1990. Measurement of changes in ligament tension
10 514 with knee motion and skeletal maturation. J Biomech Eng. 112(1):46–51.
11
12 515 Yang NH, Canavan PK, Nayeb-Hashemi H, Najafi B, Vaziri A. 2010. Protocol for constructing subject-
13 516 specific biomechanical models of knee joint. Comput Methods Biomech Biomed Engin. 13(5):589–
14 517 603.
15
16 518 Yoo YS, Jeong WS, Shetty NS, Ingham SJM, Smolinski P, Fu F. 2010. Changes in ACL length at different
17 519 knee flexion angles: An in vivo biomechanical study. Knee Surgery, Sport Traumatol Arthrosc.
18 520 18(3):292–297.
19
20 521 Zaylor W, Stulberg BN, Halloran JP. 2019. Use of distraction loading to estimate subject-specific knee
21 522 ligament slack lengths. J Biomech [Internet]. 92:1–5.
22 523 <https://doi.org/10.1016/j.jbiomech.2019.04.040>
23
24
25
26 524
27
28 525
29 526

527 Figure Captions

528 **Figure 1.** Schematic illustration for (a) kinematic test: position of tripod markers in Polaris coordinate
529 system (CSYS), (b) biplanar X-ray: 3D digital models of bone and tripod markers giving anatomical
530 and ancillary reference frames in EOS CSYS, (c) CT scan: Accurate 3D digital models of bone and
531 ligament attachment sites giving anatomical reference frames and ligament attachment locations in CT
532 CSYS, (d) knee in experimental initial configuration giving anatomical reference frames in Polaris
533 CSYS, (e) CT based subject-specific FE mesh and ligament attachment sites in experimental initial
534 configuration

535 **Figure 2.** FE model with soft tissues (only shown for the distal femur and proximal tibia region)

536 **Figure 3.** Experimental ligament length change for superficial MCL throughout the flexion movement.
537 A similar strategy was implemented for other ligaments except for PCL, which is based on literature
538 values

539 **Figure 4.** Surface representation accuracy as a Hausdorff distance for femur, tibia, and patella

540 **Figure 5.** One-to-one comparison of FE model kinematic predictions against corresponding
541 experimental data for (a) – (b): rotational and for (c) – (e): translational femorotibial kinematics
542 interpreted in femur anatomical reference frame. Results reported are based on the implementation of
543 automatically computed ligament prestrains

544 **Figure 6.** One-to-one comparison of FE model kinematic predictions against corresponding
545 experimental data for (a) – (b): rotational and for (c) – (e): translational femorotibial kinematics
546 interpreted in femur anatomical reference frame. Results reported obtained using a combination of
547 automatic pre-computation and further manual adjustment

548

1
2
3 549 **Table Headings**

4 550

5
6 551 **Table 1a** Estimated ligament stiffness values for a single specimen

7
8 552 **Table 1b** Automatically computed ligament prestrain values from experimental data (case 2)

9
10 553 **Table 1c** Prestrain obtained with a combination of automatic pre-computation and further manual
11 adjustment (case 3)

12
13 554
14 555 **Table 2** Average RMS difference \pm SD between experimental and model-predicted kinematics

15
16
17
18
19
20
21
22
23
24
25
26
27
28
29
30
31
32
33
34
35
36
37
38
39
40
41
42
43
44
45
46
47
48
49
50
51
52
53
54
55
56
57
58
59
60

For Peer Review Only

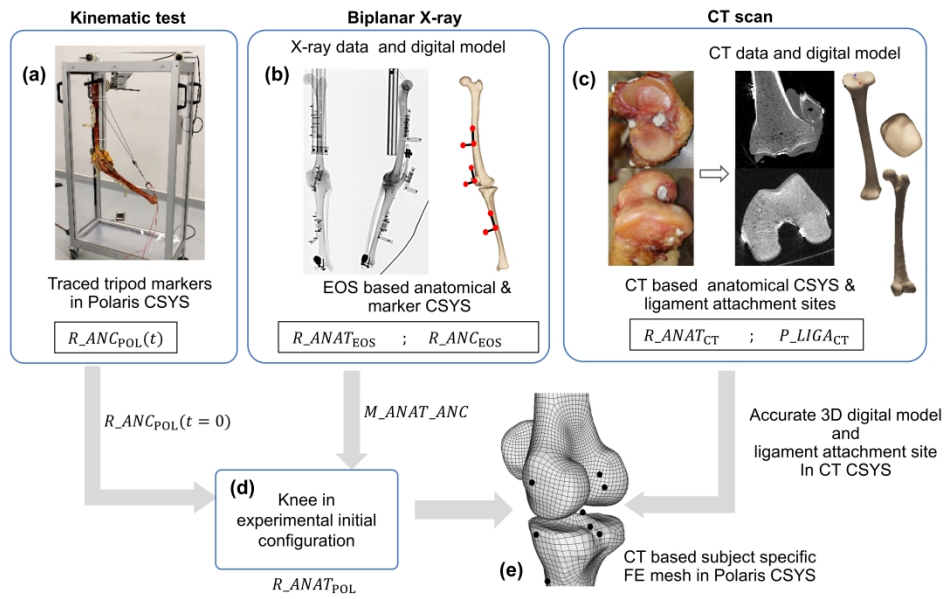


Figure 1

249x159mm (800 x 800 DPI)

1
2
3
4
5
6
7
8
9
10
11
12
13
14
15
16
17
18
19
20
21
22
23
24
25
26
27
28
29
30
31
32
33
34
35
36
37
38
39
40
41
42
43
44
45
46
47
48
49
50
51
52
53
54
55
56
57
58
59
60

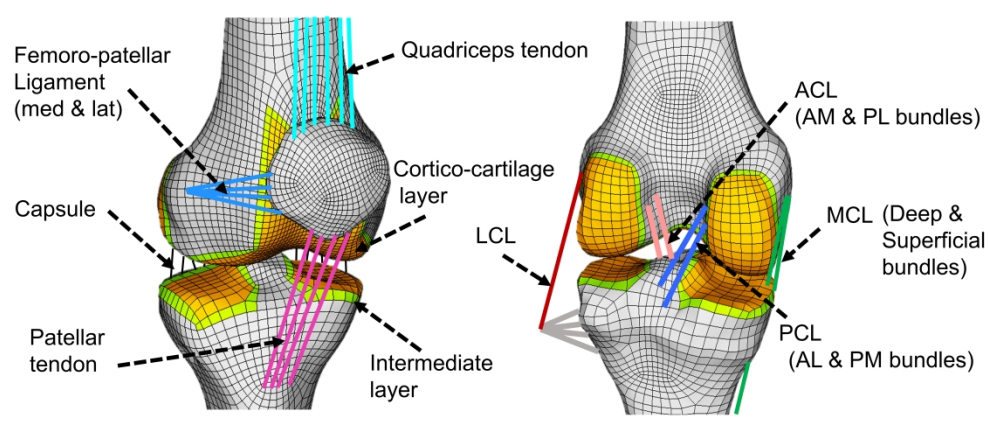


Figure 2

190x85mm (1200 x 1200 DPI)

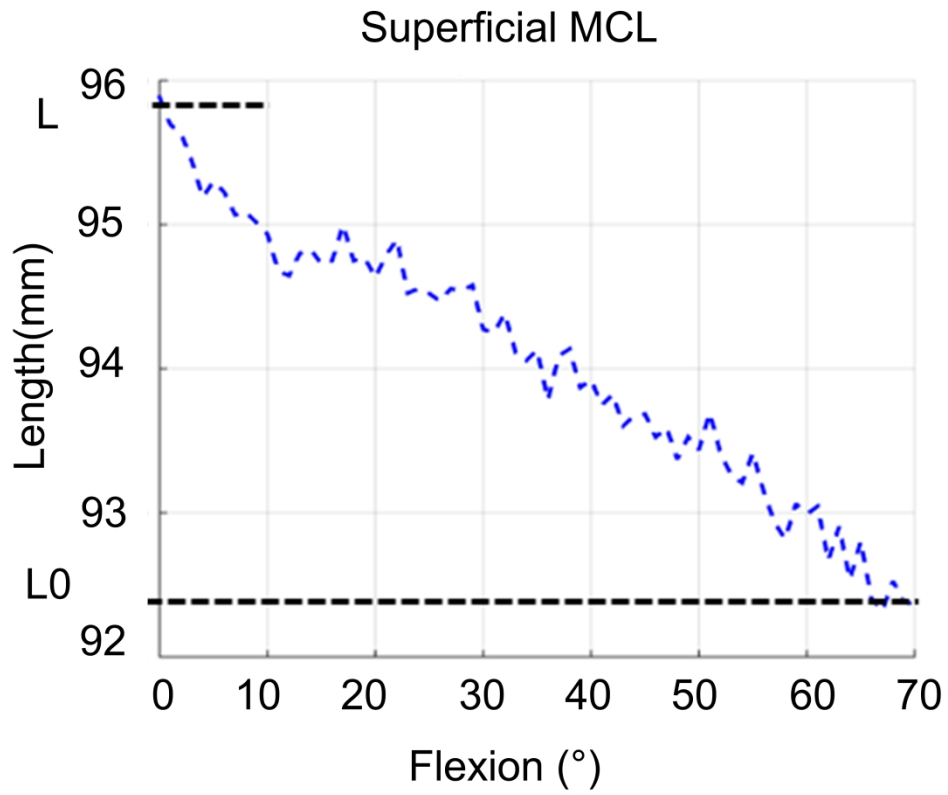


Figure 3

100x90mm (1200 x 1200 DPI)

1
2
3
4
5
6
7
8
9
10
11
12
13
14
15
16
17
18
19
20
21
22
23
24
25
26
27
28
29
30
31
32
33
34
35
36
37
38
39
40
41
42
43
44
45
46
47
48
49
50
51
52
53
54
55
56
57
58
59
60

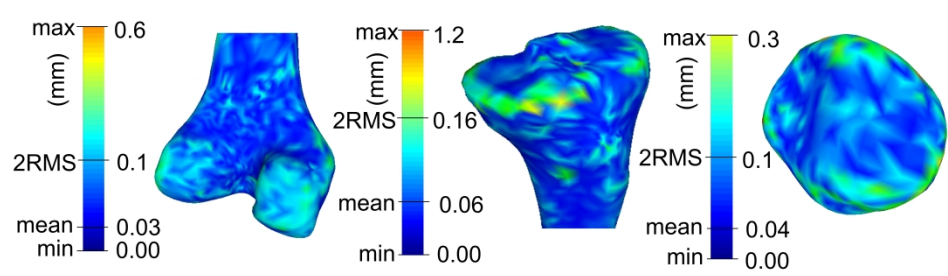


Figure 4

215x65mm (1200 x 1200 DPI)

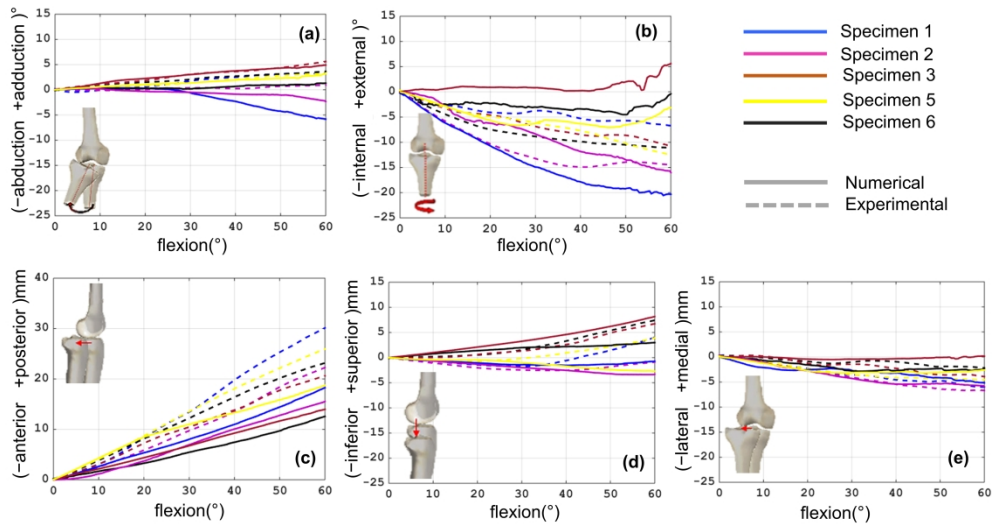


Figure 5

239x134mm (600 x 600 DPI)

1
2
3
4
5
6
7
8
9
10
11
12
13
14
15
16
17
18
19
20
21
22
23
24
25
26
27
28
29
30
31
32
33
34
35
36
37
38
39
40
41
42
43
44
45
46
47
48
49
50
51
52
53
54
55
56
57
58
59
60

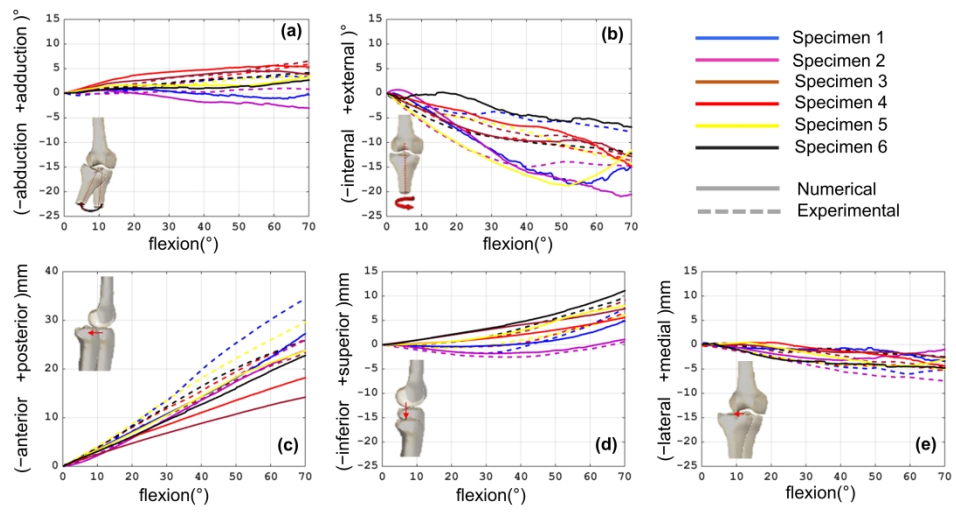


Figure 6

239x134mm (600 x 600 DPI)

Table 1a

Ligaments	ACL		PCL		MCL		LCL
Bundles	AM	PL	AL	PM	MCLd	MCLs	
Stiffness(N/mm)	125	105	125	65	45	25	60

Table 1b: Case 2

Specimens	ACL		PCL		MCL		LCL
	AM	PL	AL	PM	MCLd	MCLs	
Specimen1	8	14	-8	-20	-1	-3	10
Specimen2	6	17	-17	-3	10	5	10
Specimen3	-8	16	-10	-10	3	2	8
Specimen4	4	20	-16	-15	6	2	10
Specimen5	9	20	-15	-6	8	4	7
Specimen6	0	13	-9	4	-3	-2	9

Prestrain (%)

Table 1c: Case 3

	Ligaments & Bundles	ACL		PCL		MCL		LCL
		AM	PL	AL	PM	MCLd	MCLs	
Prestrain (%)	Specimen1	8	10	-2	-8	8	3	6
	Specimen2	6	12	-8	-4	6	3	5
	Specimen3	8	10	-8	-8	2	1	4
	Specimen4	10	10	-9	-5	2	3	6
	Specimen5	10	13	-5	-5	3	2	2
	Specimen6	6	6	-3	-3	4	3	3

Table 2

Flexion	Case	Abd/Add in°	Ext/Int in°	Post/Ant in mm	Sup/Inf in mm	Lat/Med in mm
	1	-	-	-	-	-
0 – 60°	2	2.4 ± 1.3	6.3 ± 6.2	5.0 ± 3.5	1.9 ± 1.8	1.2 ± 1.1
	3	1.5 ± 1.3	5.3 ± 5.1	3.4 ± 2.3	1.2 ± 0.8	2.0 ± 1.9